Carrier Phase Multipath Calibration of GPS Reference Stations

Lambert Wanninger, Manja May
Geodetic Institute, Dresden University of Technology, Germany

Proc. ION GPS 2000, Salt Lake City UT, 132-144.

BIOGRAPHY

Lambert Wanninger received his Dipl.-Ing. and his Dr.-Ing. in Geodesy from the University of Hannover, Germany in 1988 and 1994, respectively. He is currently employed at the Geodetic Institute, Dresden University of Technology, Germany, where he works in the field of precise GPS applications.

Manja May is a research assistant at the Geodetic Institute, Dresden University of Technology, Germany. She received a Dipl.-Ing. in Geodesy at this institute in 2000 and is involved in GPS post-processing software development since then.

ABSTRACT

Based on available GPS reference network observations we developed, implemented and tested a procedure to estimate carrier phase multipath corrections. This procedure consists of three steps: detection and localization of multipath affected satellite signals, daily estimations of multipath errors, and combination of these daily estimates to corrections for undifferenced L_1 and L_2 phase measurements.

We examined the variability of carrier phase multipath effects over one year in order to estimate the influence wetness and snow have on the reflectors. Whereas on days with continuous rainfall our multipath corrections worked as well as usually, on some days with snow cover multipath errors were altered.

In order to prove the successful calibration and correction of carrier phase multipath errors, we compared the double-differenced residuals of short and of long baselines for both uncorrected and corrected observations. Multipath errors could be significantly reduced for often used linear combinations of the dual-frequency observations, but not for the original L_1 and L_2 observations themselves. The reason can be found in the small multipath effects compared to a larger influence of remaining ionospheric errors in the multipath corrections.

1 INTRODUCTION

Precise (cm-accurate) positioning requires the use of the GPS carrier phase observables. In regional reference station networks, which provide the opportunity to very precisely model and correct distance dependent errors (ionospheric and tropospheric refraction, orbit errors, see e.g. Wanninger 1999), carrier phase multipath errors are the dominant error source for many applications.

Multipath errors occur if the received signal is composed of the direct line of sight signal and one or more indirect signals reflected in the surroundings of the receiving antenna. The occurrence of multipath depends primarily on the reflectivity of the antenna environment. If the antenna is kept at the same position and the surroundings stay unchanged, multipath errors are merely a function of the azimuth and elevation of the satellites. Hence, multipath estimations can be extracted from previous observation data and they can then be applied to correct current observations.

Recent advances in receiver technology resulted in improved mitigation of code multipath. No such improvements, however, could be achieved for carrier phase multipath, because its maximum effects occur even for very short excess signal paths (less than 1 m) where essentially no mitigation is possible (Weill 1997). More important are methods based on an appropriate processing of the carrier phase data. One such approach consists in multipath calibration of GPS reference stations.

The quality of carrier phase multipath calibration depends very much on the ability to separate multipath effects from other errors. With closely spaced antennas this presents no difficulties, since carrier phase multipath is the dominant error source. Furthermore, with antenna distances of several centimetres, multipath effects are highly correlated between antennas and can thus be estimated and eliminated (Brown and Wang 1999, Ray 1999).

In our approach, the GPS antennas are separated by several tens of kilometres and thus each station has its own multipath characteristics. Moreover, distance dependent error sources (especially ionospheric refraction, but also tropospheric refraction and orbit errors) dominate the error budget. These errors have to be modeled and reduced first, in order to be able to extract multipath information from the GPS network observations.

The German networks of GPS reference stations consist of dual-frequency receivers with station distances of about 50 km. All stations are equipped with geodetic type antennas. The observation data are available in RINEX-format with time delays ranging from a few minutes to 24 h. The default epoch rate is 15 s. No S/N-values are provided with the observations.

Our objective was to estimate carrier phase multipath corrections for these reference stations exclusively from existing data. No additional GPS sites (not even temporarily) were established. We also had no access to S/N-values, which can provide valuable information for multipath detection and estimation (Axelrad et al. 1994).

We developed a purely post-processing software solution based on existing carrier phase observations. It provides multipath corrections which then can be applied to current observations in real-time. The calibration procedure consists of three steps: detection and localization of multipath affected satellite signals, daily estimations of multipath errors and combination of these daily estimates to obtain corrections for undifferenced L_1 and L_2 phase measurements. The algorithm was implemented into the post-processing software WaSoft of the Geodetic Institute, Dresden.

2 MULTIPATH EFFECTS ON LINEAR COMBINATIONS

The carrier phase multipath error ε_M due to a single reflected signal component can be described as a function of the excess signal path (multipath delay), the ratio of direct signal amplitude to indirect signal amplitude (damping factor) and the carrier wavelength (Georgiadou and Kleusberg 1988b):

$$\varepsilon_M = \frac{\lambda}{2\pi} \cdot \arctan \frac{\alpha \cdot \sin(\frac{d}{\lambda} \cdot 2\pi)}{1 + \alpha \cdot \cos(\frac{d}{\lambda} \cdot 2\pi)} \qquad (1)$$

with

α - damping factor which varies between 0 and 1,
d - multipath delay [m],
λ - carrier wavelength [m].

Using the maximum value of the damping factor ($\alpha = 1$), the carrier phase error can reach 0.25 λ, i.e. 4.7 cm or 6.1 cm for L_1 or L_2, respectively.
For precise relative positioning, linear combinations of the original phase measurements play an important role with regard to ambiguity resolution and coordinate estimation. These linear combinations are formed using

$$L_x = a_x \cdot L_1 + b_x \cdot L_2 \qquad (2)$$

with

L_1, L_2 - observable, residual or error of original signal [m],
a_x, b_x - coefficients,
L_x - observable, residual or error of linear combination [m].

The widelane L_W with its coefficients

$$a_W = \frac{f_1}{f_1 - f_2} \text{ and } b_W = -\frac{f_2}{f_1 - f_2}$$

is essential for fast and on-the-fly ambiguity resolution. The ionosphere-free linear combination L_0 with its coefficients

$$a_0 = \frac{f_1^2}{f_1^2 - f_2^2} \text{ and } b_0 = -\frac{f_2^2}{f_1^2 - f_2^2}$$

is used for coordinate estimation of baselines longer than 5 or 10 km in order to eliminate ionospheric effects. And the geometry-free (ionospheric) linear combination L_I with the coefficients $a_I = 1$ and $b_I = -1$ is often used for ambiguity resolution of short baselines with negligible ionospheric effects.

Forming these linear combinations, multipath effects are amplified. Simulated carrier phase errors based on equations (1) and (2) are shown in Figure 1, whereas real double-differenced observations of a short baseline with the signals of one satellite at one station being multipath contaminated are presented in Figure 2. The sizes of the simulated and observed multipath effects agree very well. Maximum multipath errors increase by factors of 2 to 9 compared to their effects on the original carrier phase observations.

Looking at the same real multipath errors but now for the double-differences of a 30 km baseline, the difficulties of long baseline multipath determinations become visible (Fig. 2). Multipath is no longer the dominant error source. Relative ionospheric refraction effects caused by medium-scale variations of the ionospheric electron content can produce larger errors. Only the ionosphere-free

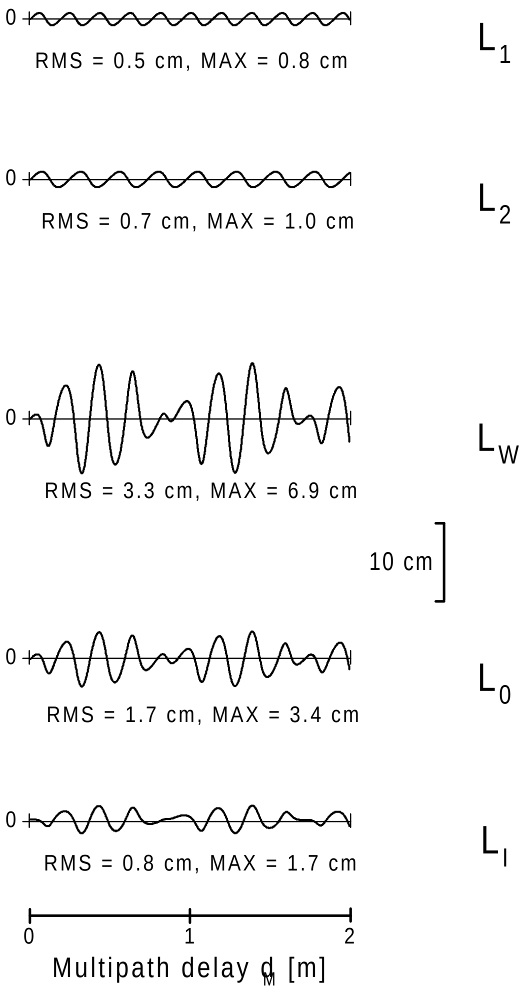

Fig. 1: Simulated carrier phase multipath errors ε_M as a function of multipath delay computed for a damping factor α of 0.25.

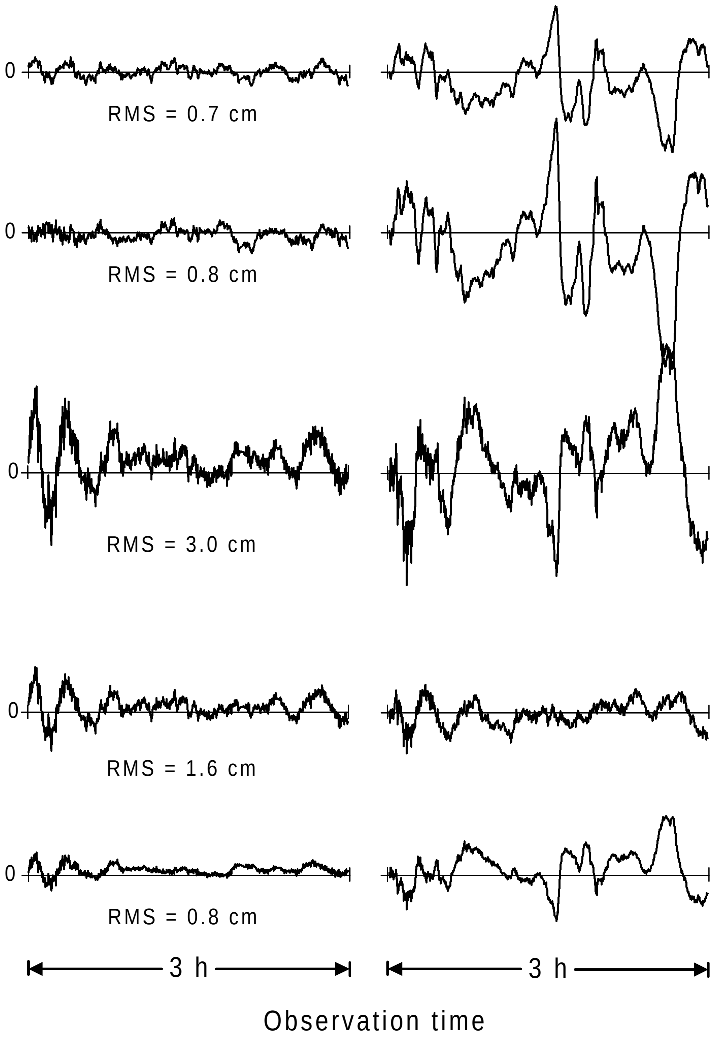

Fig. 2: Multipath errors e_M of one GPS signal, shown in double-differenced residuals of a short baseline (1 km, left) and a long baseline (30 km, right). In the long baseline remaining ionospheric effects are the dominant error source.

linear combination shows variations of carrier phase errors similar to those of the short baseline.

Medium-scale ionospheric disturbances, which are the most common form of ionospheric irregularities in mid-latitudes, mainly occur during daylight hours in winter months in years of maximum solar activity (Wanninger 1999). They cause variations in relative positioning with periods ranging from 10 minutes to one hour and thus in the same frequency range as multipath effects. A separation of these two effects in the frequency domain is therefore impracticable. Unlike multipath, the relative ionospheric errors do not repeat and can thus be averaged out using observations of several days. Nevertheless, the quality of multipath calibration in long baselines depends on the intensity of medium-scale ionospheric disturbances.

3 GPS SATELLITE ORBITS

Multipath effects depend on the geometry of the satellites, the reflectors in the vicinity of the receiving antenna, and the position of the receiving antenna itself. It can be expected that multipath effects repeat with identical geometry of the satellite, the receiving antenna and the signal reflectors.

As seen from any location on the Earth's surface, the GPS orbits repeat after about one sidereal day, i.e. 24 h minus 236 s. Therefore, multipath corrections can be stored as a function of satellite number and time forming multipath templates (e.g. Bishop et al. 1994, Kee and Parkinson 1994).

In preparation of our own correction model we estimated the offset δ [s] of the time of two complete satellite revolutions from one mean solar day (= 86400 s) using

$$\delta = 86400 - \frac{4\pi}{n} \tag{3}$$

with

n - corrected mean motion [rad/s] calculated from the GPS broadcast orbit parameters (see ICD-GPS-200 1997).

The satellite specific variations of δ for the complete year of 1999 are shown in Figure 3. We found an average δ-value of 245.6 s, which agrees very well with the results of other research groups (Seeber et al. 1998). But we also detected large outliers for two satellites which were moved within the GPS-constellation. Commencing day 30/1999 SV (PRN) 1 moved to a higher orbit and thus it needed half a minute longer to complete two revolutions. SV8 was shifted to a lower orbit about day 275/1999 and was thus 1.5 minutes per day faster than the other satellites.

Another important aspect for longer term multipath corrections are the variations of the satellite orbits with respect to the observing station. We computed all azimuth-elevation angles under which the satellites could be observed in 1999 (Fig. 4). Corresponding to the satellite velocities of Figure 3, the variations of satellite orbits as seen from the receiving antenna are fairly small. The azimuthal variations at an elevation angle of 15 deg do not exceed 3 deg for most satellites. SV1 and SV8, however, encountered much larger variations. They scanned the sky with an azimuthal drift of up to 0.2 deg/day (SV1) or up to 0.5 deg/day (SV8). For these scanning satellites, multipath corrections have a very short effective lifetime of a few days. On the other hand, especially these satellites provide very useful information for a complete map of the multipath effects of a GPS reference station.

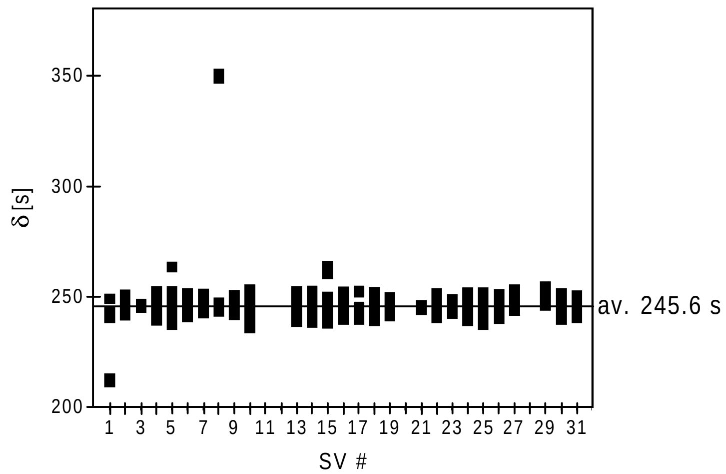

Fig. 3: GPS satellite velocities for 1999 shown as offsets δ of the time of two complete satellite revolutions from one mean solar day.

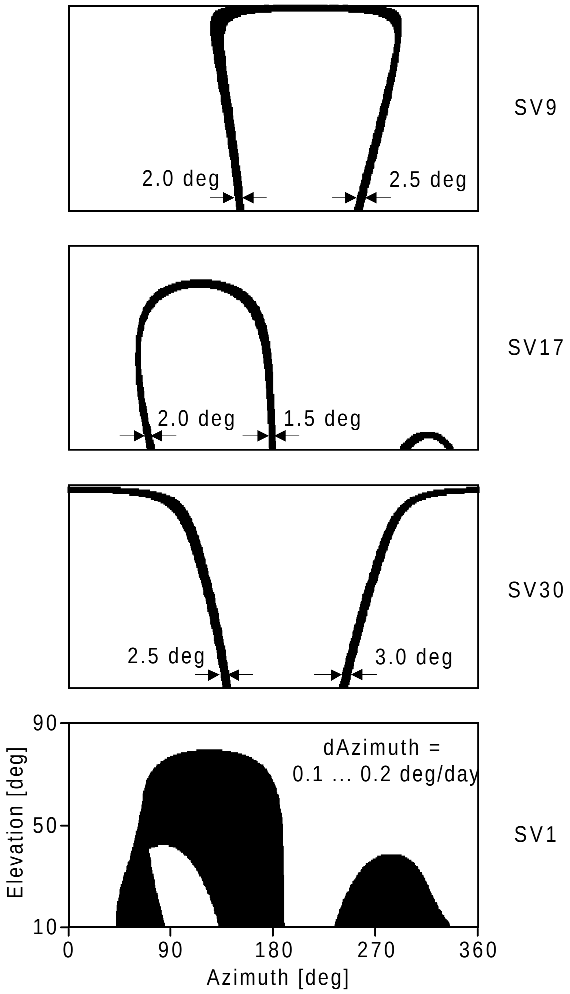

Fig. 4: Azimuth-elevation coverage of selected GPS satellites for a Central European station in 1999.

In order to be independent of these peculiarities of the GPS orbits, we decided not to use multipath template techniques. We rather consider multipath errors to be a function of the direct signal incidence angle and thus map multipath corrections in a coordinate system of azimuth and elevation.

4 DETECTION AND LOCALIZATION OF CARRIER PHASE MULTIPATH

Multipath effects can be detected in time series of double-differenced residuals of the carrier phase observables. The ionosphere-free linear combination is especially suitable for multipath detection since it is much more affected by multipath than the original signals (cf. Fig. 1 and 2). Furthermore, detection can be performed even in baselines longer than a few kilometers due to the elimination of ionospheric refraction effects.

The detection algorithm is based on the following characteristics of multipath effects:

- The dominant multipath periods range from 10 to 45 minutes mainly dependent on the distance reflector-antenna. Since ionospheric refraction has been eliminated by forming the ionosphere-free linear combinations no other error source with a similar characteristic remains.
- Due to the location of the GPS-antennas on top of roofs all reflectors are situated below the antenna horizon and thus we can expect that satellite signals incident from low elevations (e.g. below 50 deg) are affected and signals coming from higher elevations (e.g. above 50 deg) show little effects.
- Multipath effects are uncorrelated between reference stations since each roof and antenna position has its individual characteristic.

The detection and localization algorithm consists of the following steps:

- Compute undifferenced residuals of the ionosphere-free linear combination (similar to producing carrier phase corrections according to RTCM (1998)).
- Form 20 minute blocks of data of low elevated (below 50 deg) satellites and test them individually using the following three steps:

– Form double-differenced residuals from undifferenced data using the observations to be tested, simultaneous observations of the highest elevated satellite at the same station and the corresponding observations at the other stations in the network. This results in (n-1) vectors of double-differenced observations in a network of n stations (Fig. 5).

– Reduce each vector by the average value of all its elements in order to remove the carrier phase ambiguities, remaining tropospheric effects and the influence of orbit errors. If the standard deviations of the majority of vectors exceed a predefined limit (e.g. 15 mm), multipath can be suspected (Tab. 1).

– Correlate the vectors of double-differenced observations in all combinations. If the majority of correlation coefficients exceeds a predefined limit (e.g. 0.8) the detected multipath effects are caused by the undifferenced observations to be tested (Tab. 1).

Please note that this algorithm does not require any ambiguity fixing to integer values nor does it produce any better results after replacing the broadcast ephemerides by precise ephemerides.

An example of multipath detection and localization is presented in Figure 5 and Table 1. A 20 minute block of observations of the signal of a specific satellite observed from station A is tested against the observations of seven other stations in the network. The standard deviations of the seven double-difference vectors exceed 15 mm with one exception (baseline A-C). 67 % of the correlation coefficients are larger than 0.8 and thus multipath effects were detected and the causing undifferenced observations (satellite, station) could be identified.

The smaller standard deviation and correlation coefficients for baseline A-C are caused by multipath effects for the same satellite but at station C. The multipath effects at A and at C for this satellite and in this period of 20 minutes are very similar and thus they largely cancel out in the double-differences which results in a small standard deviation.

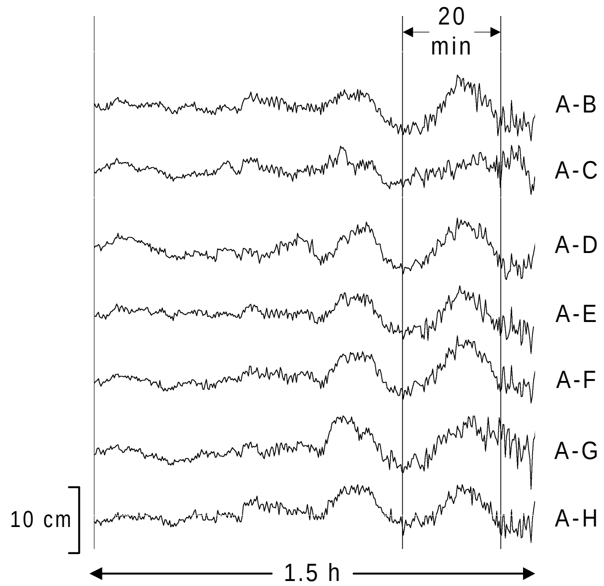

Fig. 5: Ionosphere-free double-differenced residuals for a satellite below 50 deg of elevation observed from station A. These residuals were formed using the observations of a satellite above 50 deg of elevation to be assumed multipath-free and the corresponding observations at the stations B to H.

Tab. 1: Standard deviations and correlation coefficients for the 20 minute time period indicated in Figure 5.

Base-line	Stddev. [mm]	Correlation Coefficients A-C	A-D	A-E	A-F	A-G	A-H
A - B	31	.66	.95	.94	.96	.80	.95
A - C	14	-	.73	.67	.70	.73	.67
A - D	27	-	-	.94	.97	.82	.94
A - E	26	-	-	-	.93	.80	.93
A - F	30	-	-	-	-	.83	.95
A - G	27	-	-	-	-	-	.78
A - H	23	-	-	-	-	-	-

The example shows that this detection and localization algorithm requires a majority of unaffected signals in order to be able to identify the affected ones. Fortunately, the strongly affected stations within the German reference networks comprise only about 20 % of all stations (Wanninger and Wildt 1997).

Furthermore, we can subdivide the detection and localization procedure. In a first step all stations of a network are processed simultaneously in order to separate severely affected from slightly affected stations. In the second step the slightly affected stations are processed separately and each severely affected station is tested against the group of slightly affected stations.

Our experiences with this detection and localization algorithm show that in reference station networks with station separations of some 50 km reliable results can already be obtained with single 24 h data sets (60 s data rate). In order to verify the results we usually repeat the procedure with a second 24 h data set. In general, the differences between two independent detections are negligible.

Having identified a multipath affected portion of a signal, azimuth and elevation of the transmitting satellite are stored in gridded form with a rectangular resolution of 2 deg (elevation) x 10 deg (azimuth). For each bin an average standard deviation value based on the double-difference standard deviations is produced in order to give an indication of the intensity of the multipath errors.

Our test network consists of 9 stations owned by the State Survey Department of Sachsen-Anhalt, Germany. We applied our multipath detection algorithm to the network observation data of 1999. Since no considerable day-to-day variations of detected multipath could be observed, the daily detection grid maps were combined to station maps (Fig. 6).

Five stations can be considered as (almost) multipath-free (BITT, LOBU, LUW2, SAN2, WEI2), some multipath effects could be detected for two stations (HALW, STAF) and the signals of the remaining two stations are severely affected (DESS, MAGD). This agrees with our earlier results that about 20 % of the German reference stations

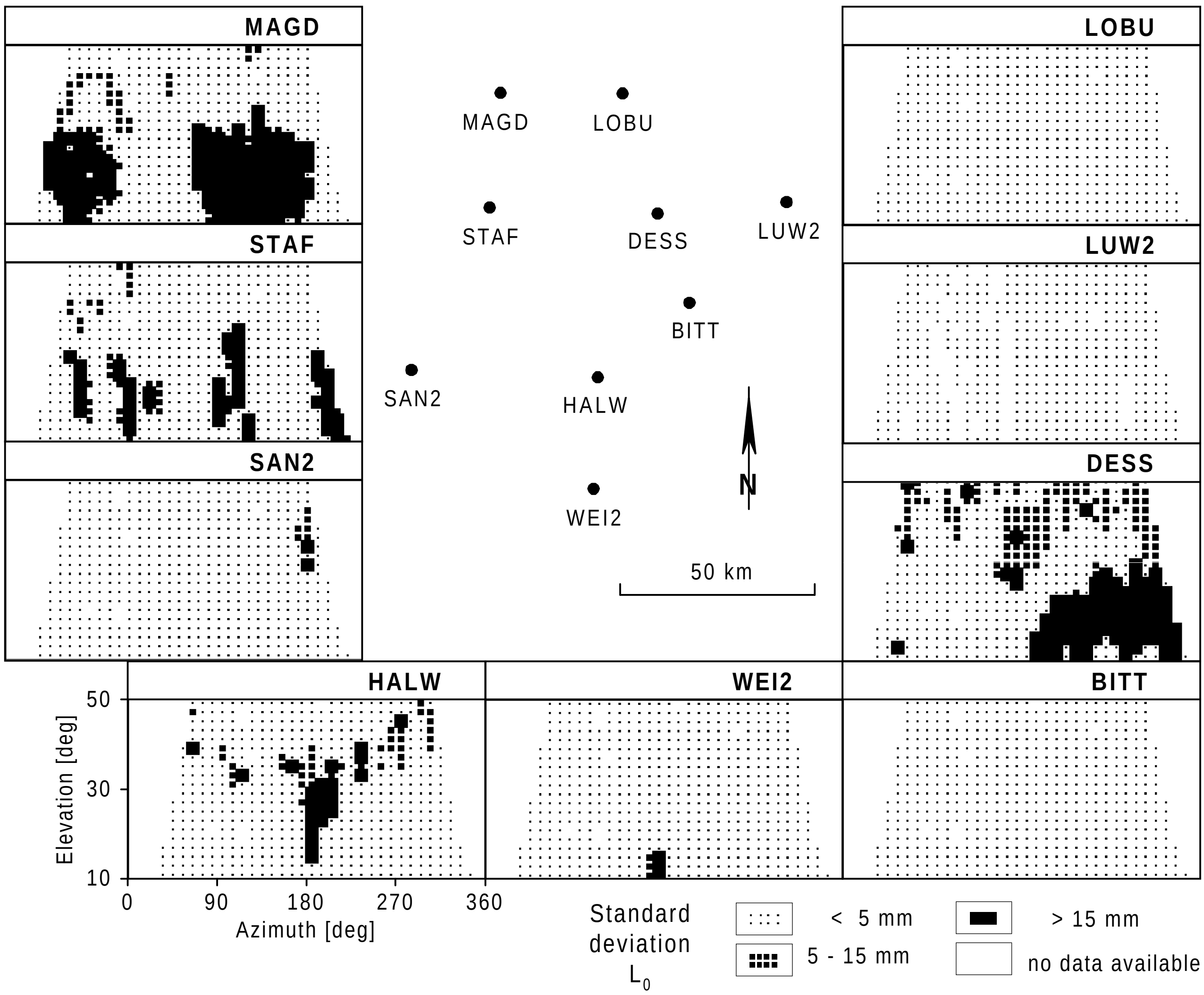

Fig. 6: GPS reference station network consisting of 9 stations, multipath detection results for each station.

suffer from severe carrier phase multipath effects. A majority of stations is (almost) multipath-free and can thus be used to determine multipath corrections for the severely affected stations.

5 CARRIER PHASE MULTIPATH CALIBRATION

In order to be able to determine carrier phase multipath corrections, ambiguity resolution is required in all baselines of the network. Since the coordinates of the reference stations are precisely known and data processing can be performed in post-processing, ambiguity resolution presents no real difficulty.

We store and handle the carrier phase observations in undifferenced mode. Compared with a single-difference approach we have the advantage that after ambiguity resolution the observations of all stations and satellites are on the same ambiguity level, i.e. we can easily form ambiguity-free double-differenced observables between any stations and satellites.

For both, ambiguity resolution and multipath correction, we try to keep the effects of distance dependent errors as small as possible. From the geometry-free linear combination of the carrier phase data we estimate a single-layer model of the vertical ionospheric electron content VEC in a coordinate system of geographic latitude φ and local time t (cf. Georgiadou and Kleusberg 1988a)

$$VEC(\varphi,t) = a_{00} + a_{10} \cdot (\varphi - \varphi_0) + a_{01} \cdot (t - t_0) + a_{02} \cdot (t - t_0)^2 \tag{4}$$

with

a_{ij} - model coefficients,
φ_0, t_0 - coordinates of the selected origin of a local coordinate system.

This yields the observations equation of the geometry-free (ionospheric) linear combinations of carrier phase data:

$$L_I = m_I \cdot VEC(\varphi,t) + C_I^i \,. \tag{5}$$

It contains the ionospheric mapping function m_I, the Vertical Electron Content at the intersection of the signal path with the ionospheric layer and satellite-individual constants C_I which absorb the undifferenced carrier phase ambiguities and differential hardware delays.

We estimate sets of the VEC model coefficients by least squares adjustment for observation times of 3 hours and apply the ionospheric corrections to the undifferenced L_1 and L_2 observations. With these models we are able to considerably reduce the effects of large-scale features of the ionosphere. But we are not able to remove the effects of medium-scale ionospheric features. They present the main error source in multipath calibration in regional GPS networks.

Tropospheric corrections are applied according to a standard atmospheric model. Additionally, residual zenith delays are calculated from the GPS network data. We estimate one zenith delay parameter per station for each 4 hours of observations. The estimated tropospheric corrections are then applied to the undifferenced L_1 and L_2 observations.

The introduction of precise IGS orbits had essentially no effect on the ambiguity resolution nor it noticeably improved the estimated multipath corrections. Hence, we worked with the GPS broadcast orbits only.

After ambiguity resolution and mitigation of the distance dependent error, multipath corrections are estimated for each L_1 and L_2 observation separately according to the following double-difference algorithm. Multipath estimations are performed only for those selected stations S and selected satellites s, for which multipath errors were detected with L_0 standard deviations larger 15 mm (cf. Fig. 6). Reference satellites j are all those satellites with elevations larger 50 deg. We assume that their signals are not affected by multipath. All those stations without any detected multipath (L_0 standard deviation below 5 mm) for satellite s serve as reference stations I. Multipath estimates e_M are then obtained from

$$e_M = \frac{1}{\Sigma w} \cdot \sum_{I=1}^{N} \sum_{j=1}^{m} (r_S^s - r_S^j - r_I^s + r_I^j) \cdot w_{SI} \tag{6}$$

with

r - undifferenced L_1 or L_2 carrier phase residuals with double-differenced ambiguities resolved and ionospheric and tropospheric correction applied as described above

and a weighting factor

$$w_{SI} = \frac{1}{d_{SI}} \tag{7}$$

as a function of the distance d_{SI} between the selected station S and the reference station I.

The multipath estimates are stored together with an identifier for station S, azimuth and elevation of satellite s and time.

In a subsequent step we estimated multipath corrections in gridded form. We tested several pixel sizes ranging from 0.1 deg x 0.1 deg to 1 deg x 1 deg in azimuth and elevation. Since we could not detect improved multipath correction with higher resolution, we ended up using the most storage-saving resolution of 1 deg x 1 deg. Basically, we average all those multipath estimates which fall into the same pixels. A two step approach allows us to detect outliers and remove them from further data processing.

Calibration maps can now be produced based on different amounts of multipath estimates ranging from a single day to several days or even a whole year.

6 1999 CALIBRATION RESULTS

The multipath detection within our test network revealed that 2 out of 9 reference stations show some multipath effects and another 2 stations are severely affected by carrier phase multipath (cf. Fig. 6). We applied the calibration algorithm described above to all affected stations, but restrict the presentation of results to the most affected stations DESS and MAGD.

In order to be able to present a complete picture of multipath corrections, we calculated multipath estimates e_M not only for those 2 deg x 10 deg detection pixels with L_0 standard deviations larger 15 mm but for all observations below 50 deg elevation angle. Using the observations of the whole year of 1999 and averaging the estimates e_M within each 1 deg x 1 deg calibration pixel yields L_1 and L_2 calibration maps (Fig. 8). The corresponding calibration maps for linear combinations were calculated using equation (2).

No calibration values can be obtained for northern directions, because no GPS satellite signals are received from this part of the sky. Some smaller gaps can be observed around 90 deg and 200 deg of azimuth, where no signals were incident in 1999. These remaining gaps are fairly small, because of the scanning satellites SV1 and SV8. We obtained multipath correction values for 69 % of all 1 deg x 1 deg pixels between 10 and 50 deg of elevation. Without the two scanning satellites, the percentage would have been only 23. This, however, is no drawback to multipath calibration, because no corrections are needed for those incident angles without satellite signals.

The GPS antennas at both stations DESS and MAGD are mounted on roofs. No obstructions or reflectors exist above the antenna horizons (Fig. 7). Hence, only the roofs themselves need to be considered as potential reflectors.

In the case of DESS, the roof right below the antenna (the upper roof in Fig. 7) expands from 170 deg in azimuth to northern direction. Within this azimuth range and for elevations below 30 deg large multipath corrections were determined (Fig. 8). Their wavelike pattern with a wavelength of about 7 deg in elevation indicates that the reflector is located very close to the antenna. Since the roof is tilted to east direction the multipath waves are bent with an elevation maximum at about 270 deg in azimuth.

At DESS no significant multipath corrections were obtained for signals from low elevated satellites within the azimuth range from 30 to 160 deg. This agrees very well with the multipath detection results (cf. Fig. 6) and can easily be explained from the antenna surroundings. Because the antenna is mounted close to the eastern edge of

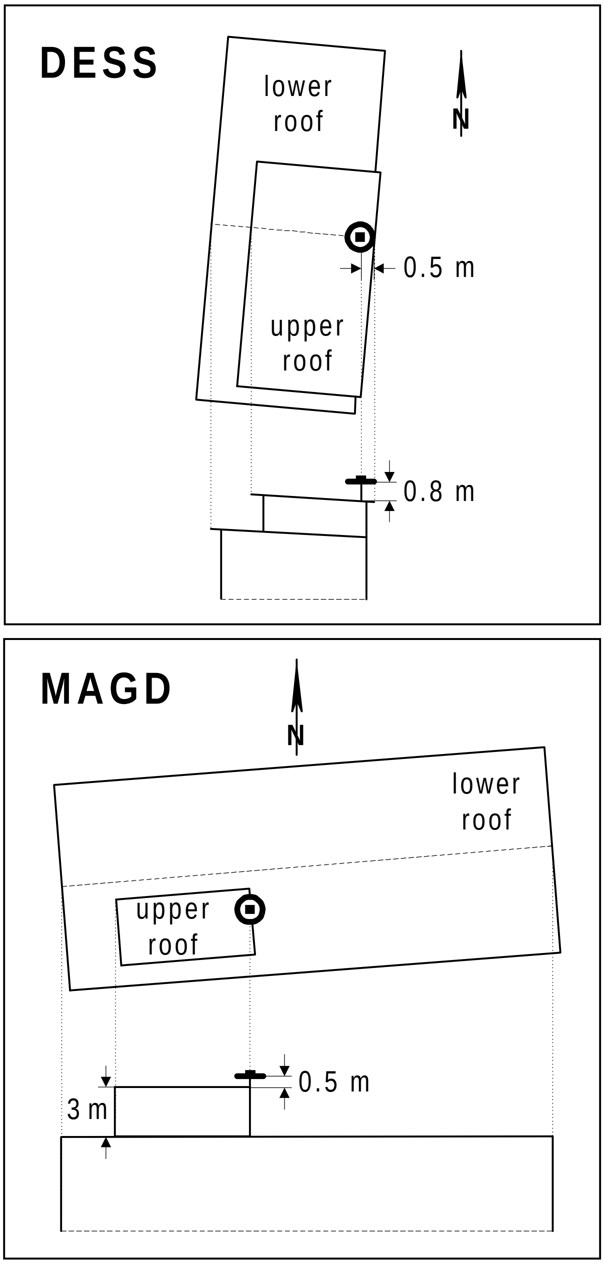

Fig. 7: The surroundings of the GPS reference antennas at DESS and at MAGD.

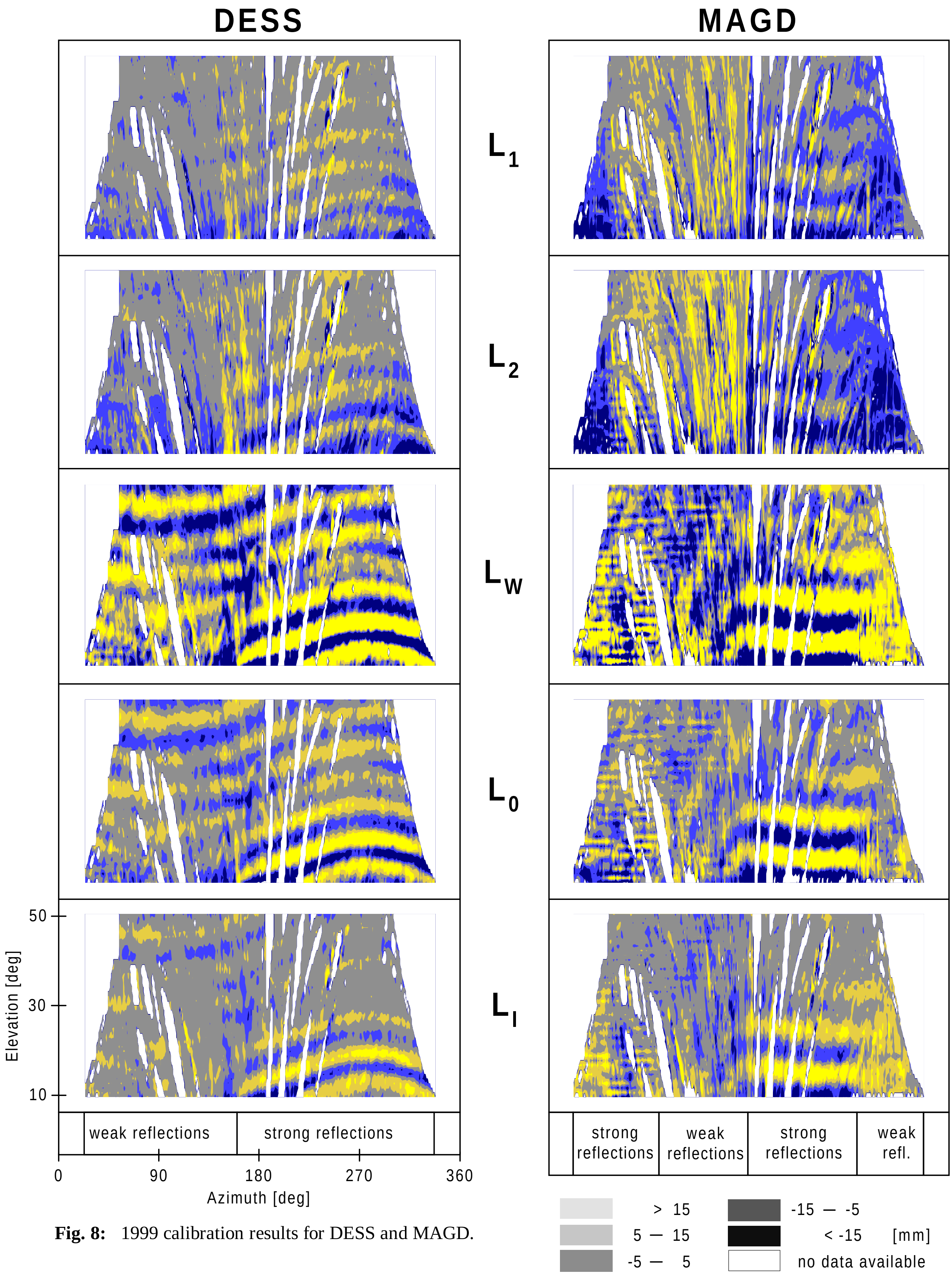

Fig. 8: 1999 calibration results for DESS and MAGD.

the roof, no reflectors exist for signals incident from low elevations. The signals coming from elevations above 40 deg, however, are affected by multipath, which can only be originated from the small roof strip between antenna and roof edge. They as well had already shown up in the detection results (Fig. 6).

At MAGD two reflector surfaces exist: a lower roof in a distance of a few meters and an upper roof right below the antenna (Fig. 7). Since both surfaces are flat, i.e. not tilted, the multipath patterns are constant for constant elevations. The wavelengths of the multipath patterns in elevation amounts to about 7 deg for the upper roof (azimuth range from 160 to 280 deg) and to about 2.5 deg for the lower roof (from 0 to 160 deg).

Looking at the calibration maps of different linear combinations, earlier findings are confirmed that in the original L_1 and L_2 observations multipath signals have small amplitudes and are thus difficult to detect. Other linear combinations like widelane L_W, ionosphere-free signal L_0 and even the geometry-free signal L_I are much more affected.

7 DAY-TO-DAY VARIABILITY OF MULTIPATH EFFECTS

An important aspect of multipath calibration is the variability of carrier phase multipath effects with environmental changes in the antenna vicinity. In our case, typical changes may be caused by rain and snow which are expected to affect the reflectivity of the roof surfaces.

In order to test the validity of multipath corrections we produced L_1 and L_2 calibration maps for DESS from all the 1999 data. In contrast to Figure 8, we now determined correction values only for pixels with a detected multipath strength of more than 15 mm L_0 standard deviation (cf. Fig. 6).

We determined daily solutions for the baseline DESS-BITT (24 km) with the original DESS observations and also with multipath corrected observations. The least squares adjustment provides the standard deviation of the observables as an indicator for the size of observations errors. Comparing these indicators of the daily solutions with and without multipath corrections shows how effective multipath correction works for this 24 km-baseline. Negative percentage values in Figure 9 indicate mitigation of multipath effects. The average improvement is very small for L_1 and L_2 (less than 1 %) but reaches significant values for the three linear combinations L_W, L_0, and L_I.

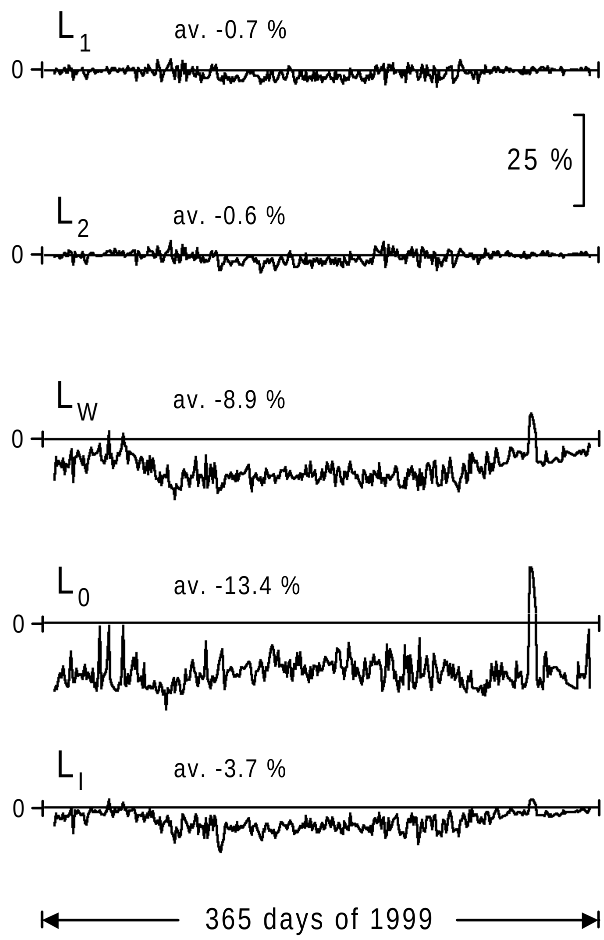

Fig. 9: The effect of multipath corrections on the overall observation errors in the 24 km-baseline DESS-BITT. Negative values indicate a reduction of observation errors due to multipath corrections.

Please note that multipath corrections were applied to only 9 % of all DESS observations, namely to the most affected ones. A correction of all observations within an elevation range of 10 to 50 deg (70 % of all observations) further reduces the errors in L_0 and L_W but significantly deteriorates the L_1 and L_2 solutions.

Looking at the day-to-day variability of the observation error reduction, it can be noticed that a seasonal variation exist in all those signals which are affected by the ionosphere, i.e. in all signals except L_0. This effect can be explained by the influence of medium-scale ionospheric disturbances which mainly occur in winter time. Due to the larger relative ionospheric errors at the beginning and at the end of 1999, multipath causes a smaller portion of the overall error budget and thus multipath mitigation has smaller effects.

Furthermore, some outliers can be detected, especially in the ionosphere-free linear combination L_0 on the following 8 days: 32, 38, 48, 324 to 328 and 364. We checked the weather records of that area and found that on 6 of these 8 days temperatures were below 0°C and snowfall was reported. Unfortunately, we are not able to precisely verify whether or not the roof or the antenna were covered with snow. Nevertheless, there are strong indications that these outliers were caused by snow. No similar conclusion can be drawn for variations due to rainfall and thus the wetness of the reflectors. Continuous rainfall was reported for 23 days but no effects can be found in the multipath mitigation results.

8 APPLICATION OF MULTIPATH CORRECTIONS TO FURTHER TEST DATA

A further test data set was observed end of May 2000. In direct vicinity to the reference station DESS, three GPS receivers were employed at stations almost free of any multipath effects**.** 24 hours of observations were collected. The objective of this test consisted in proofing the effectiveness of multipath corrections obtained from a regional network of GPS reference stations and applied to short baselines.

Double-differenced carrier phase residuals of the short baselines (1 km) to DESS served as multipath indicator. Since no distance dependent error sources can produce significant errors on these short baselines, multipath is the dominant error source for all signals. Comparing double-differenced residuals before and after multipath correction of the observations collected at DESS, provides a good estimate of the size of multipath mitigation.

A representative example of double-differenced residuals is presented in Figure 10. The original data clearly shows oscillating multipath errors which disappear after application of multipath corrections. RMS-values of double-differenced residuals are reduced by 30 to 50 % in widelane L_W, ionosphere-free L_0 and geometry-free L_I linear combinations. The original L_1 and L_2 observations, however, show no improvements and even worse, double-differenced residuals in L_2 are amplified.

Averaged standard deviations for all baselines from the three local stations to DESS provide similar results. Here, we also tested several kinds of correction models, with the results of three models being presented in Table 2. We were interested in how many days of multipath estimates are needed to produce a good calibration result. Hence, we estimated corrections from an increasing number of previous days.

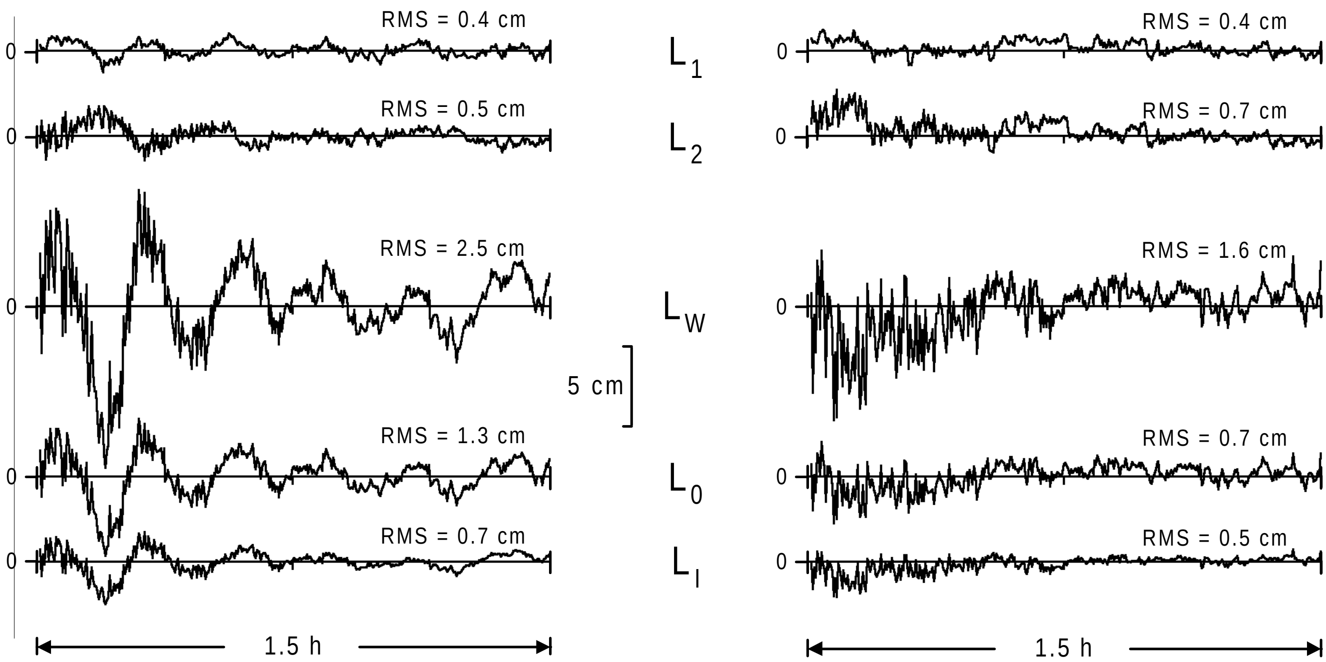

Fig. 10: Mitigation of multipath effects in a short baseline: shown are double-differenced residuals and RMS-values before (left) and after (right) multipath correction.

Tab. 2: Short baseline (1 km) standard deviations of observation residuals.

[mm]	L_1	L_2	L_W	L_0	L_I
uncorrected	3.5	5.0	20.2	10.0	5.3
corrected with model based on data of ...					
previous day	5.0	7.1	17.7	8.9	4.9
previous 10 days	3.5	5.1	17.2	8.5	4.6
year 1999	3.9	5.8	17.0	8.3	4.7

Tab. 3: Long baseline (24 km) standard deviations of observation residuals.

[mm]	L_1	L_2	L_W	L_0	L_I
uncorrected	21.9	34.8	33.3	11.7	26.9
corrected with model based on data of ...					
previous day	22.4	35.4	31.9	10.9	26.6
previous 10 days	22.0	34.9	31.6	10.7	26.4
year 1999	22.1	35.0	31.5	10.6	26.4

With a single previous day we already see improvements in the linear combinations, but ionospheric errors deteriorate the L_1 and L_2 results. With 10 days of multipath estimates L_1 and L_2 standard deviations are as large as without corrections but significant improvements can be achieved in the linear combinations. No further improvements could be achieved using multipath estimates of more than 10 previous days. Applying the 1999 calibration model to the May 2000 data produces results almost as good as with multipath estimates of the previous days. Unfortunately, L_1 and L_2 observations deteriorate again.

We performed the same tests for a 24-hour sample of the 24 km long baseline DESS-BITT (Tab. 3). Here, remaining ionospheric refraction is the dominant error source for all signals except the ionosphere-free linear combination L_0. The model based on the multipath estimates of 10 previous days produces the best results. The corrections from 1999 are of similar quality.

The tests show that we are able to considerably reduce observation errors in the linear combinations L_W, L_0, and L_I for reference stations being affected by large multipath errors. On the other hand, no improvements could be achieved for L_1 and L_2. We even have to carefully tune our calibration algorithm so that no additional (ionospheric) errors are introduced into the L_1 and L_2 observables.

8 CONCLUSION

We were able to extract carrier phase multipath corrections from the observations of a regional GPS network. The calibration algorithm consists of three distinct steps: detection, localization, and calibration of carrier phase multipath. The corrections are applied to the undifferenced observations of the reference stations.

The variability of carrier phase multipath over one year revealed that large variations could be observed on days with snow cover on the reflectors (or snow cover on the antenna ?). No such variations could be attributed to rainfall and thus the wetness of the reflectors.

Multipath errors could significantly be reduced in widelane L_W, ionosphere-free L_0 and geometry-free L_I linear combinations. No such improvements could be achieved for the L_1 and L_2 signals, because multipath affects these signals much less than linear combinations based on these signals. In L_1 and L_2 remaining ionospheric errors in our multipath correction models cancel any improvements due to multipath mitigation.

It can be expected that the shorter the station distances in the reference station network, the better multipath mitigation results can be expected using the described algorithm.

ACKNOWLEDGEMENTS

The GPS reference station observations were made available by the State Survey Department of Sachsen-Anhalt, Halle, Germany.

REFERENCES

Axelrad, P., Comp, C., MacDoran, P. (1994): Use of Signal-to-Noise Ratio for Multipath Error Correction in GPS Differential Phase Measurements: Methodology and Experimental Results. Proc. ION GPS 94, Salt Lake City, UT, 655-666.

Bishop, G.J., Coco, D.S., Kappler, P.H., Holland, E.A. (1994): Studies and Performance of a New Technique for Mitigation of Pseudorange Multipath Effects in GPS Ground Stations. Proc. ION 94 National Tech. Meeting, San Diego, CA, 231-242.

Brown, A., Wang, J. (1999): High Accuracy Kinematic GPS Performance Using a Digital Beam-Steering Array. Proc. ION GPS 99, Nashville, TN, 1685-1693.

Georgiadou, Y., Kleusberg, A. (1988a): On the Effect of Ionospheric Delay on Geodetic Relative GPS Positioning. Manuscripta Geodetica **13**:1-8.

Georgiadou, Y., Kleusberg, A. (1988b): On Carrier Signal Multipath Effects in Relative GPS Positioning. Manuscripta Geodaetica, **13**:172-179.

ICD-GPS-200 (1997): Interface Control Document: NAVSTAR GPS Space Segment / Navigation User Interfaces, ARINC Research Corporation, El Segundo, CA.

Kee, C., Parkinson, B. (1994): Calibration of Multipath Errors on GPS Pseudorange Measurements. Proc. ION GPS 94, Salt Lake City, UT, 353-362.

Ray, J.K. (1999): Use of Multiple Antennas to Mitigate Carrier Phase Multipath in Reference Stations. Proc. ION GPS 99, Nashville, TN, 269-279.

RTCM (1998): RTCM Recommended Standards for Differential GNSS Service, Version 2.2. RTCM Paper 11-98/SC 104-STD, Alexandria VA.

Seeber, G., Menge, F., Völksen, C., Wübbena, G., Schmitz, M. (1998): Precise GPS Positioning Improvements by Reducing Antenna and Site Dependent Effects. IAG Scientific Assembly, Rio de Janeiro, 1997, IAG Proc. Vol. 118, 237-244.

Wanninger, L., Wildt, S. (1997): Identifikation von Mehrwegeeinflüssen in GPS-Referenzstationsbeobachtungen. Allgemeine Vermessungs-Nachrichten (AVN), **104**:12-15.

Wanninger, L. (1999): The Performance of Virtual Reference Stations in Active Geodetic GPS-Networks under Solar Maximum Conditions. Proc. ION GPS 99, Nashville, TN, 1419-1427.

Weill, L.R. (1997): Conquering Multipath: The GPS Accuracy Battle. GPS World, April 1997, 59-66.